Cell, Vol. 69, 963–975, June 12, 1992, Copyright © 1992 by Cell Press

The *argos* Gene Encodes a Diffusible Factor That Regulates Cell Fate Decisions in the Drosophila Eye

Matthew Freeman,* Christian Klämbt,† Corey S. Goodman, and Gerald M. Rubin
Howard Hughes Medical Institute
Department of Molecular and Cell Biology
University of California
Berkeley, California 94720

Summary

The *argos* gene encodes a protein that is required for viability and that regulates the determination of cells in the Drosophila eye. A developmental analysis of *argos* mutant eyes indicates that the mystery cells, which are usually nonneuronal, are transformed into extra photoreceptors, and that supernumerary cone cells and pigment cells are also recruited. Clonal analysis indicates that *argos* acts nonautonomously and can diffuse over the range of several cell diameters. Conceptual translation of the *argos* gene suggests that it encodes a secreted protein.

Introduction

Communication between cells has emerged as a theme underlying many of the mechanisms by which cells in a developing organism acquire their specific fate. A cell may receive information from its neighbors, causing it to adopt a specific identity and thereby to follow a particular developmental pathway (Amaya et al., 1991; Artavanis-Tsakonas and Simpson, 1991; Horvitz and Sternberg, 1991). These cell–cell interactions can be limited to adjacent cells, or can be over a longer range, mediated by a diffusible factor. Inductive interactions have been extensively studied in the Drosophila compound eye, which comprises about 750 identical unit eyes, or ommatidia (Tomlinson, 1988; Ready, 1989). Each ommatidium contains 8 photoreceptor cells and 12 nonneuronal cells. Differentiation of the ommatidia begins during the third larval instar in a monolayer epithelium known as the eye imaginal disc. Within the imaginal disc, a given cell's fate is known to be independent of its ancestry, and is believed to be determined only through interaction with other cells (Lawrence and Green, 1979; Wolff and Ready, 1991).

An example of an interaction between adjacent cells that has been well characterized in the developing Drosophila eye is the determination of the photoreceptor cell R7. The R7 cell requires a signal from the adjacent cell, R8, in order to differentiate, and this interaction is mediated by the products of the *sevenless* gene, a receptor tyrosine kinase, and the *boss* gene, the ligand for *sevenless* (Hafen et al., 1987; Krämer et al., 1991). Examples of longer range cell-to-cell communication mediated by diffusible molecules occur in a variety of systems. In some cases diffusible molecules appear to have a direct role in cell fate determination (see, e.g., Smith et al., 1990; van den Eijnden-van Raaij et al., 1990; Amaya et al., 1991). In Drosophila, these include the products of the *decapentaplegic* and *wingless* genes (Baker, 1987; van den Heuvel et al., 1989; Panganiban et al., 1990; Posakony et al., 1990), although the latter appears to act locally, perhaps only with immediately neighboring cells. In the Drosophila eye the scabrous protein, which is secreted, has a role in regulating the spacing of the ommatidia, through a process known as lateral inhibition (Baker et al., 1990; Mlodzik et al., 1990a). Apart from scabrous, no diffusible factors believed to influence photoreceptor determination have been identified in the Drosophila eye.

In this paper we describe a newly identified gene, *argos*. Phenotypic analysis of *argos* mutations in the developing eye suggests that it is a diffusible negative regulator of inductive signals that specify cell fate, and it appears to be able to act over a range of at least several cell diameters. This view is supported by the fact that the sequence of the *argos* gene indicates that the protein is secreted. Our data suggest that the induction of cell fate in the eye can involve an interplay between opposing positive and negative regulatory signals.

Results

argos^{W11} Is a Recessive Mutation That Disrupts Eye Development

The *argos*^{W11} mutation is a P element insertion that was isolated in an enhancer trap screen (see Experimental Procedures). Flies homozygous for this allele show reduced viability and have an extreme rough eye phenotype, including blistering in the posterior region of the eye (Figure 1). This contrasts with the regular array of ommatidia that can be seen in a wild-type Drosophila eye. The internal structure of the wild-type eye can be seen clearly in semithin sections. Each ommatidium comprises 8 photoreceptor cells and 12 nonneuronal support cells. The photoreceptors are easily identified by their specialized light-trapping organelles, the rhabdomeres. Eyes of *argos*^{W11} flies have abnormal rhabdomere morphology and extra outer photoreceptors (Figure 1D). All the rhabdomeres are smaller than wild type, and they degenerate rapidly after eclosion. In sections through 1 hr old flies, it is apparent that most ommatidia have one or two extra photoreceptors, but by the time the flies are more than 2 days old, there are no identifiable rhabdomeres (Figure 1E). The optic lobes of *argos*^{W11} flies are small and disorganized.

The Development of *argos*^{W11} Eyes

In order to understand the abnormal phenotype of *argos*^{W11} adult eyes, we have followed their development from the time when the cells are first determined (Figure 2). Eye

*Present address: Medical Research Council, Laboratory of Molecular Biology, Hills Road, Cambridge CB2 2QH, England.
†Present address: Institut für Entwicklungsbiologie, Universität zu Köln, Gyrhofstrasse 17, 5000 Köln 41, Germany.

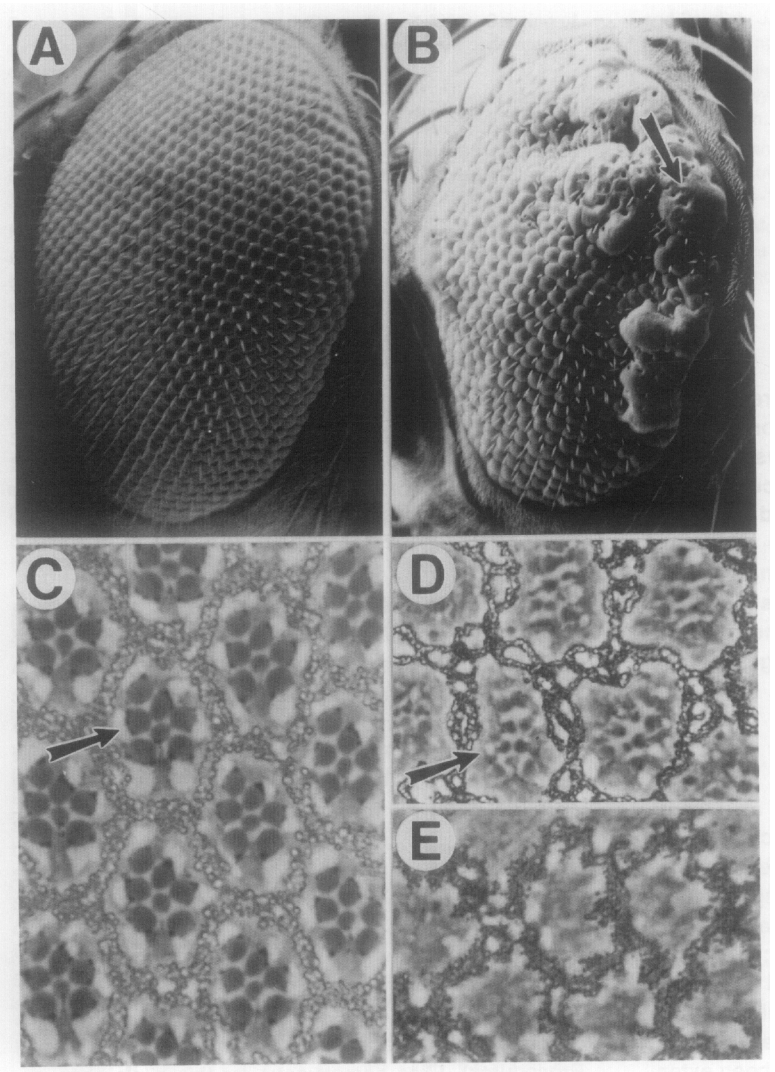

Figure 1. The *argos* Eye Phenotype

(A) A scanning electron micrograph of a wild-type Drosophila eye. Note the regular array of facets, or ommatidia.

(B) In the *argos*^{W11} mutant eye, the regular array is disrupted, causing a severe roughening of the eye. The posterior region shows characteristic blistering (arrow).

(C) A 2 μm tangential section through the wild-type eye allows the internal structure of the ommatidia to be seen. Each has eight photoreceptors, of which seven can be seen in any one plane of section, and these are easily identified by their rhabdomeres, which are seen as dark projections forming an asymmetric trapezoid (see arrow). The ommatidia are surrounded by an array of pigment cells, which produce the refractive pigment granules that form a honeycomb lattice.

(D) A section through an *argos*^{W11} eye from a fly less than 1 hr old. Although the photoreceptors are small and abnormally formed, it can be seen that most ommatidia have one or two extra rhabdomeres; the arrow indicates an ommatidium with nine visible rhabdomeres. The poor morphology makes it difficult to obtain a precise number for the proportion of ommatidia with extra cells, but it is about 70%, which corresponds well to the proportion in the middle of large *argos* clones.

(E) A section through a 5 day old *argos*^{W11} eye: no rhabdomeres are visible, and the photoreceptors have apparently degenerated.

development starts during the third instar larva, in a monolayer epithelium called the eye imaginal disc. An indentation, the morphogenetic furrow, sweeps across the disc, and as cells emerge from the posterior of this furrow, they start to show signs of differentiating: they undergo morphological changes and express neural antigens (for detailed description, see Tomlinson, 1988; Ready, 1989). A consequence of this mode of development is that a single eye disc contains developing ommatidia of different ages, ranging from the most immature ommatidia immediately behind the furrow to much older ones near the posterior of the disc.

When stained with antibodies that recognize neural antigens, the overall morphology of the *argos*^{W11} eye imaginal disc appears relatively normal: using antibodies against neural markers, the sequence of early neuronal differentiation (first cell 8, then 2 and 5, and 3 and 4) appears normal, although we cannot rule out subtle defects at this earliest stage of ommatidial assembly (Figures 2A–2F). The first abnormality that we have detected occurs a few rows posterior to the morphogenetic furrow. Many of the clusters in *argos*^{W11} discs have extra neural cells, and some are abnormally oriented. This is most clearly seen at the stage when the wild-type disc has five cells expressing neural antigens in a "precluster" (cells 8, 2, 5, 3, and 4). In *argos*^{W11} discs one or two extra neural cells are often seen (Figures 2E and 2F). The position of these additional cells is adjacent to cells R3 and R4, where the "mystery cells" reside

Figure 2. The Development of *argos*^{W11} Eyes

(A–F) Wild-type third instar eye imaginal discs (A–C) and *argos*^{W11} discs (D–F), stained with antibodies against ubiquitous neuronal antigens (A, B, D, and E, anti-neuroglian [Hortsch et al., 1990]; C and F, 22C10 [Fujita et al., 1982]); we have also used an antibody against Elav (Bier et al., 1988; Robinow and White, 1991), another ubiquitous neuronal antigen, and we obtain similar results (data not shown). Although the *argos* disc appears normal at low power (compare A and D; arrow marks position of the morphogenetic furrow), closer examination shows that there are frequently

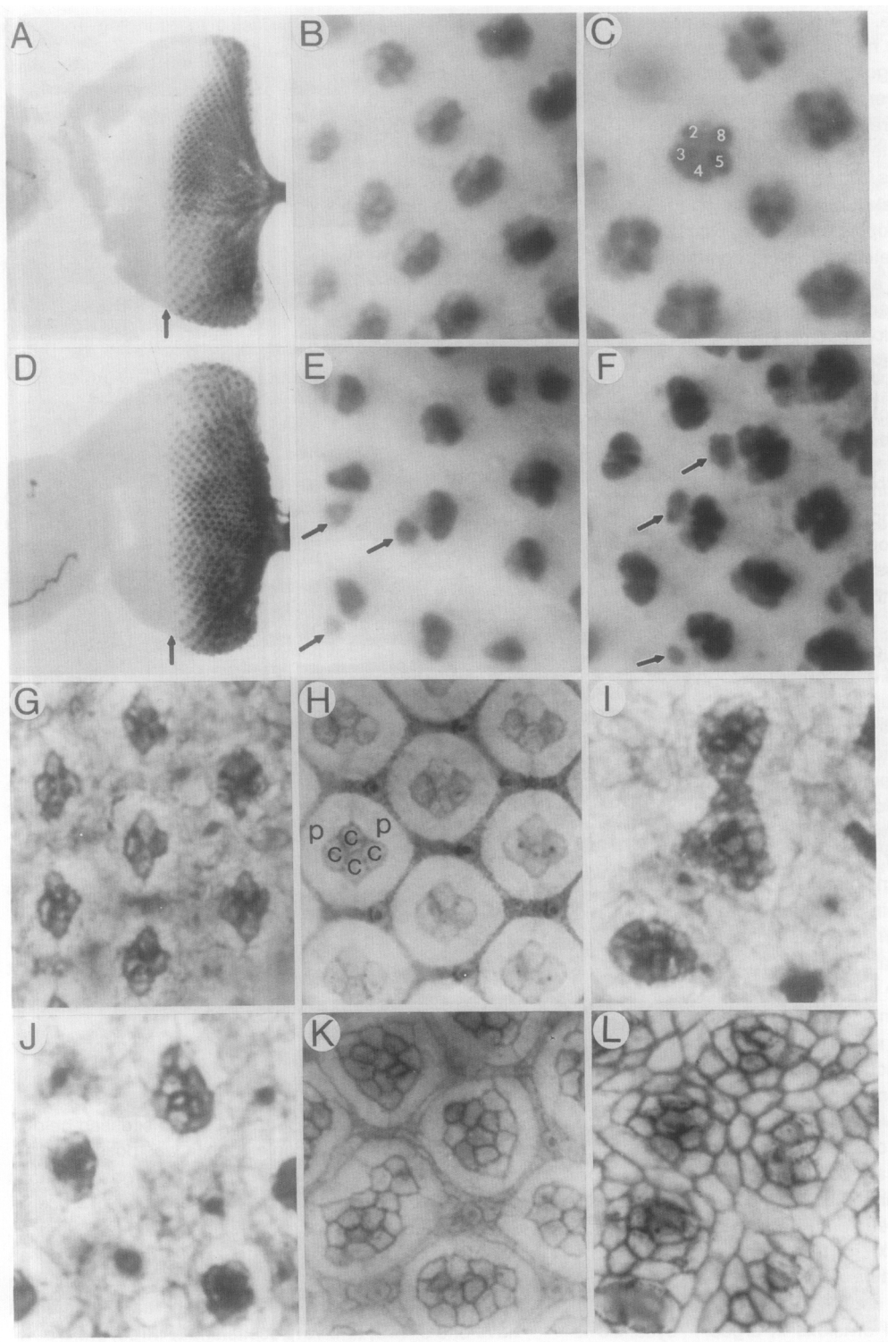

one or two extra neuronal cells per ommatidium in the mutant discs, indicated in (E) and (F) by arrows. At a time when 3 and then 5 cells are differentiating in the wild-type discs (cells 8, 2, and 5 and then 3 and 4—see C), the extra cells can be seen in the characteristic mystery cell position, adjacent to cells 3 and 4. These transformed mystery cells start to express neuroglian and the 22C10 antigen a little before cells 3 and 4. In (B), (C), (E), and (F), the morphogenetic furrow is to the left. A significant number of ommatidia are also abnormally oriented (see E for example).
(G–L) Cobalt sulfide stained retinae of wild-type (G and H) and *argos*^{W11} (I–L) pupal retinae. (G) By 21 hr of pupal development, four cone cells are seen in wild-type ommatidia, whereas extra cone cells have been recruited in mutant retinae (J). (H) At 40 hr, wild-type ommatidia still have four cone cells (c), and two primary pigment cells (p) surround them; in comparison, 40 hr *argos*^{W11} ommatidia (K) have many extra cone cells (up to 20, average ≈ 9) and also extra primary pigment cells (usually 3 or 4 cells in total). (I) A pair of ommatidia beginning to fuse in a 24 hr *argos*^{W11} retina; approximately 5–10 such fusions are seen in a typical retina. (L) A region from the posterior of a 35 hr *argos*^{W11} retina, in which there are no primary pigment cells; later, no discrete ommatidia are seen in these regions of the adult eye.

in wild-type eye discs. The mystery cells are so called because their fate in normal development is unknown. They appear to undergo the earliest stages of ommatidial differentiation; however, they never express neural antigens, they leave the precluster soon after they are identifiable, and their ultimate fate is unclear (Tomlinson et al., 1987). In *argos*^{W11} discs it appears that many of the mystery cells inappropriately start differentiating as neurons and never leave the developing ommatidia. Occasionally, extra neural cells are detected between ommatidia, rather than associated with a specific cluster. It is not known whether these represent rare cases of different cells undergoing neural development, or whether a mystery cell sometime breaks away from its parental cluster.

We have shown that there is extra neural recruitment in the third larval instar of *argos*^{W11} imaginal discs. In order to discover whether there were additional later defects, we also examined pupal eye development. This was done by cobalt sulfide staining, which highlights the apical cell contacts in the developing retina (Melamed and Trujillo-Cenoz, 1975). All the cells apart from the photoreceptors have apical projections at this stage. From early in pupal eye development, further defects are found in *argos*^{W11} flies (Figures 2G–2L). The most striking of these is that there are many more cone cells than normal. The cone cells are nonneuronal and contribute to the structure of the lens. By 21 hr of pupal development it is apparent that nearly all ommatidia have more than the normal four cone cells overlying their photoreceptors (compare Figures 2G and 2J). By 40 hr, this number has further increased, to an average of about nine cone cells per ommatidium (Figure 2K). By focusing below these clusters of cone cells, we can count the number of photoreceptors in each cluster (data not shown). We find that there are typically one or two extra photoreceptors, implying that there is no additional neural recruitment after the mystery cells are transformed. In a few cases we see as many as 20 cone cells in a single cluster. These may be the products of the ommatidial fusions that are occasionally seen (approximately 5–10 per retina; Figure 2I), and which appear to be caused by primary pigment cells encircling two adjacent clusters. The number of primary pigment cells is also abnormally high: three, four or even five can be seen to surround each ommatidium, instead of the normal complement of two (compare Figures 2H and 2K). There also appear to be extra secondary and tertiary pigment cells, although since these are shared between ommatidia, it is difficult to estimate their overall number in an eye that is so disorganized. Bristle precursors are similarly disorganized, though their total number appears about normal. We have found no evidence of extra cell divisions in *argos*^{W11} eyes, so it seems likely that the additional cells are recruited from the pool of uncommitted cells that exists in the developing eye. We have some preliminary evidence that there may be slightly fewer ommatidia formed in *argos*^{W11} discs, which could explain the increase of total number of cells per ommatidium that occurs.

In the posterior region of pupal retinae there are areas that are devoid of primary pigment cells delimiting each ommatidium. Instead there is a lawn of cells that are difficult to identify, owing to the lack of surrounding landmarks (Figure 2L). It is these regions lacking primary pigment cells that fail to form discrete ommatidia, leading to a general secretion of lens material and the formation of blisters or large ommatidial fusions in the adult eye (as seen in Figure 1B).

The defects in *argos*^{W11} eyes that we have been able to establish can be summarized as follows. From a few rows posterior to the morphogenetic furrow, extra neural cells begin to join the clusters. Later, these are joined by extra cone cells, primary pigment cells, and perhaps secondary and tertiary pigment cells as well. Our data cannot rule out other abnormalities in the earliest stages of ommatidial assembly, but the apparently normal progression of neural differentiation suggests that there are no other gross defects.

P Element Excision Mutations of *argos*

In order to determine that the insertion of the enhancer trap P element was responsible for the *argos*^{W11} phenotype, we mobilized the element and generated lines of flies from which the *white* gene had been lost. These excision lines fell into three classes: 34% (13/38) were wild type, 50% (19/38) had rough eyes, and 16% (6/38) had a lethal mutation in the same complementation group. The high rate of reversion to wild type upon excision of the P element implies that the insertion was responsible for the *argos* phenotype; if it was caused by an unrelated mutation on the chromosome, no correlation would be seen between excision of the element and reversion of the phenotype. The rough eye and lethal mutations generated by P element mobilization are caused by various types of imprecise excision events, including internal deletions and deletions of flanking genomic DNA, both of which are common events (Daniels et al., 1985).

Since the lethals generated by imprecise excision were all in the same complementation group, we reasoned that they represented mutations in the gene immediately adjacent to the P element insertion site. By mapping the extent of the deletions in these lines, we have confirmed that this is indeed the case, and that they are all small deletions that affect the 5′ end of the same gene as is disrupted by the insertion (shown in Figure 5A and discussed below).

Using mitotically induced clones, it was possible to examine the eye phenotype of these lethal *argos* mutations and to compare it with the phenotype of clones of *argos*^{W11}. This was done by producing clones of marked tissue, which were homozygous for the *argos* mutations, in an otherwise heterozygous fly. The predominant phenotype associated with these clones is that the adult ommatidia have one or two, and very occasionally three, extra outer photoreceptors (Figure 3). Frequently, the architecture of the ommatidium is not badly disrupted by the addition, and in these cases the position of the extra cells is consistent with that expected of transformed mystery cells, adjacent to cells R3 and R4. This extra cell phenotype is not fully penetrant: not all genotypically mutant ommatidia have extra photoreceptors. These observations are consistent with the imaginal disc phenotype of *argos*^{W11} described above. Importantly, no phenotypic difference can be seen

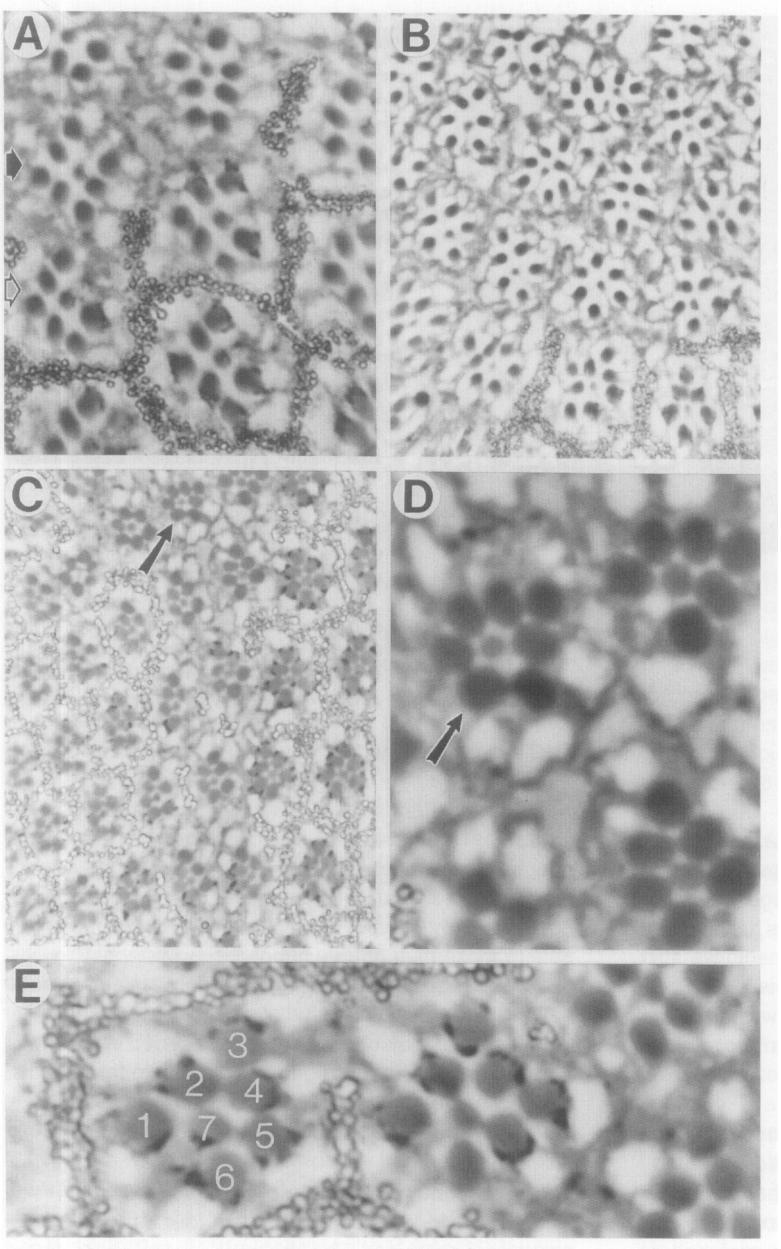

Figure 3. *argos* Clonal Analysis

Clones of the four different lethal alleles are indistinguishable. The ones shown here are from $argos^{\Lambda 3}$ and $argos^{\Lambda 5}$.

(A) The primary phenotype of *argos* clones in the eye is the formation of extra photoreceptors. Instead of the normal seven visible rhabdomeres in any plane of section, eight or nine can be seen, indicating that one or two additional photoreceptors have been recruited (compare a normal [open arrowhead] and a mutant ommatidium [closed arrowhead]). The phenotype is not fully penetrant, so that there are always some normally constructed ommatidia in *argos* clones.

(B) Large clones have a higher proportion of mutant ommatidia than small clones, especially in the center of the clone (see text).

(C–D) In long, narrow clones, very few ommatidia have extra photoreceptors. The arrow indicates a single ommatidium with an extra photoreceptor (shown enlarged in D).

(E) Some ommatidia are only slightly disrupted by the addition of an extra cell, so cell identities can be assigned with some confidence. In this section (at the R7 level), two adjacent ommatidia are shown, one normally constructed and one abnormal. In the phenotypically mutant ommatidium, only cells R6 and R7 are genotypically mutant, but it has a transformed mystery cell in a different part of the ommatidium, indicating that the transformation is nonautonomous (cell R8 is not seen in this plane of section, but is also genotypically wild type). It is important to stress that we cannot be sure which cell is the transformed mystery cell, as there may be some shuffling of the positions of cells 3, 4, and the extra cell during development; however, it is very unlikely that the extra cell, which is recruited beyond cells 3 and 4 in the disc, is one of the two *w* cells, which are on the other side of the ommatidium. Such a major reorganization would be likely to disrupt the trapezoid morphology more profoundly. We have seen several examples of this type of mosaic ommatidium.

between clones of $argos^{W11}$ (data not shown) and clones of the *argos* deletion mutations (Figure 3). This suggests that, at least in the eye, the insertion mutation and the deletions all have similar effects on the *argos* gene. Furthermore, two of the deletions remove all P element sequences, indicating that the $argos^{W11}$ mutation leads to a reduction in gene function, and that the $argos^{W11}$ phenotype is not due to misexpression of the gene caused by the insertion of the P element.

Clonal Analysis Indicates That *argos* Acts Nonautonomously

By analyzing the mitotic clones, we were able to determine whether the *argos* gene product is required in the cells in which it is expressed, or in other cells; that is, does *argos* act autonomously or nonautonomously? Our data provide clear evidence that *argos* acts nonautonomously: a cell does not need to be genotypically $argos^{-}$ in order to acquire an abnormal fate, and surrounding wild-type tissue can cause $argos^{-}$ cells to develop normally. First, the severity of the *argos* phenotype is dependent upon the size of the clone. In large clones (greater than 20 ommatidia) the proportion of ommatidia with extra photoreceptors is higher than in small clones (fewer than 10 ommatidia), and additional defects become apparent, including a loss of regular ommatidial orientation (Figure 3B). Small or long, narrow clones often have few, if any, defects (Figures 3C and 3D). Second, as is described below, genotypically mutant ommatidia close to a clone boundary are more frequently phenotypically wild type than ones in the center of

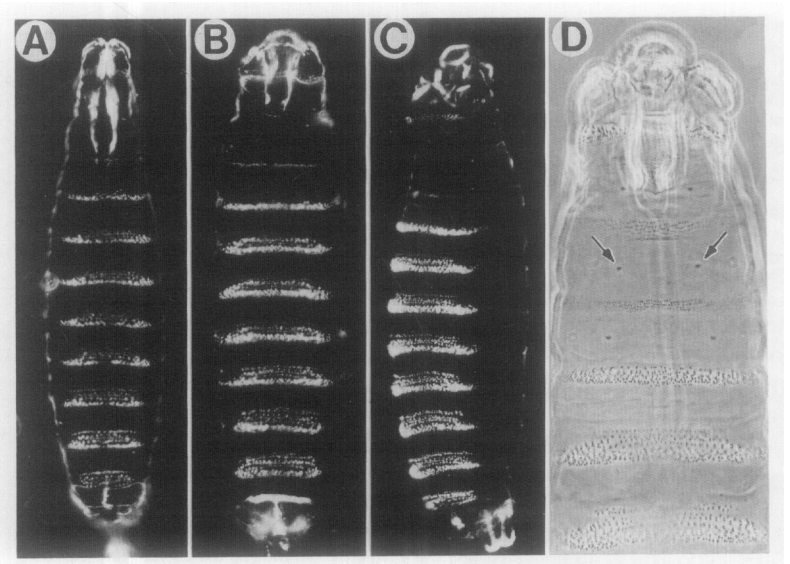

Figure 4. The Embryonic Phenotype of *argos* Lethals

(A) Cuticle of a wild-type embryo. (B) Ventral view and (C) lateral view of an $argos^{\Delta 7}/argos^{\Delta 7}$ embryonic cuticle. Note that the there are major defects in the head skeleton structure in the *argos* embryos, and that the head and ventral structures are broader than wild type. (D) An *argos* embryo, in which the Keilin's organs can be seen (arrows). The separation of the pairs of Keilin's organs is increased by 50% in *argos* lethal mutants (see Table 1). We have used molecular probes to look for evidence of this broadening in earlier embryonic stages. The *decapentaplegic* (*dpp*) gene is expressed in a stripe of cells that appears to mark the lateral boundary of the ventral epidermis (Ray et al., 1991). In situ hybridizations to wild-type and *argos* embryos show no difference in the separation of these stripes of *dpp* expression, as late as the germband extended embryo (stage 11). The disco protein is expressed in the precursor cells of the Keilin's organs (Cohen et al., 1991). Comparing the separation of these precursor cells in wild-type and *argos* embryos also shows no detectable difference, as late as the germband retracted embryo (stage 13). Thus, it appears as if the ventral expansion is a relatively late-occurring phenomenon.

a clone. Third, it is possible to find ommatidia in which the extra cell is in the mystery cell position, but the only mutant cells are in a different part of the cluster, suggesting that the extra cell itself, or its immediate neighbors, do not need to be genotypically mutant (Figure 3E). Finally, we also found a single case of a genotypically fully wild-type ommatidium on the edge of an $argos^{-}$ clone, which had an extra photoreceptor. In this case, the transformed mystery cell must be genotypically wild type.

argos Can Transmit a Signal over a Distance

In order to find out over what range the wild-type argos protein is able to rescue the extra cell phenotype, we counted the proportion of ommatidia with extra photoreceptors in different regions of a clone. We assigned all the fully genotypically mutant ommatidia from three large clones into two regions. "Clone edge ommatidia" were those that were less than two ommatidial diameters from wild-type tissue; all the rest were classed as "central ommatidia." We found that 21% (17/80) of clone edge ommatidia had extra photoreceptors, compared with 67% (72/107) of central ommatidia. About 70% of ommatidia in whole eyes from $argos^{w11}$ flies have extra photoreceptors (see Figure 1), which corresponds well to the proportion seen in the middle of large *argos* clones. Although there is some subjectivity in these regional assignments, the large difference in the proportion of phenotypically mutant ommatidia implies that the rescuing effect of wild-type tissue diminishes over the range of one or two ommatidia, that is, a few cell diameters.

Even large clones of *argos* lethal mutations or $argos^{w11}$ do not show the degeneration seen in whole eyes from $argos^{w11}$. Therefore, this necrosis may be the consequence of defects in the optic lobes, which are clearly disrupted in *argos* mutants, rather than a primary eye-dependent phenotype. If the photoreceptor axons are unable to make their normal connections with these mutant optic lobes, this could lead to the progressive degeneration throughout adult life that occurs in $argos^{w11}$. A similar adult degeneration of photoreceptors is seen in eyes from flies mutant for the *disco* gene, which fail to form normal connections between the eye and optic lobe (Campos et al., 1992; J. S. Heilig, personal communication).

The Embryonic *argos* Phenotype

Cuticles of embryos carrying any of four lethal alleles of *argos* were examined. The four mutations were generated as described above, by imprecise excision of the enhancer trap transposon. All four show a similar phenotype, and this description is based on $argos^{\Delta 7}$ homozygotes. This allele has the whole of the 5′ exon, including the beginning of the major open reading frame, deleted (see Figure 5), and so is likely to represent a null mutation. Homozygous embryos die late in development, although an occasional hatched larva is found. Examination of the cuticles of these embryos show two principal defects (Figure 4). The first is a severe, but variably expressed, disruption and broadening of the embryonic head skeleton. The second defect is a pronounced broadening of the ventral epidermis, detected in embryonic cuticle preparations. This can be measured by comparing the width of the denticle belts that traverse the ventral surface of the embryo, but is most reliably quantified by measuring the separation of the Keilin's organs, which are pairs of sensory organs that are

Table 1. Separation of the Keilin's Organs in Thoracic Segments T1–T3

	Wild Type	$argos^{\Delta 7}$	Expansion
T1	16.3 ± 0.7	27.8 ± 2.4	+59%
T2	21.6 ± 0.8	33.3 ± 2.9	+54%
T3	30.5 ± 1.1	45.4 ± 3.9	+49%

The distance between the Keilin's organs in each segment was measured on a microscope using a micrometer eyepiece.The separations are given in arbitrary units, ± standard errors. Measurements were made from 23 Oregon-R wild-type embryos and 17 $argos^{\Delta 7}/argos^{\Delta 7}$ embryos. By Student's t-test, these differences are statistically significant ($p < 0.001$).

positioned ventrolaterally in the three thoracic segments. In all *argos* lethal alleles, the distance between the pairs of Keilin's organs is increased by about 50% (Table 1).

Isolation of the *argos* Gene

The region flanking the $argos^{W11}$ enhancer trap insertion was cloned from a genomic library (Figure 5). The *argos* lethal mutations caused by the imprecise excision of the transposon were localized with respect to the *argos* transcription unit and the genomic map of the region, and they are shown in Figure 5A. $argos^{\Delta 5}$ and $argos^{\Delta 7}$ remove DNA around the 5′ end of the argos gene. $argos^{\Delta 3}$ and $argos^{\Delta 6}$ are both internal deletions within the enhancer trap P element and do not delete additional genomic sequences. These latter two cases suggest that in the $argos^{W11}$ insertion mutant (which is viable), there is some transcription of the gene directed by sequences within the P element; when these spurious promoter elements are removed by an internal deletion, the remaining P element sequences are sufficient to fully disrupt the gene, producing the lethal phenotype. DNA fragments from around the insertion point were used to screen cDNA libraries from embryos and eye imaginal discs. Several transcripts were detected, and one class of cDNAs present in both libraries was found to hybridize with the 2.6 kb restriction fragment into which the transposon is inserted. More precise mapping of this class indicated that the 5′ end of the longest cDNA (2.8 kb) was located 10 nt 3′ of the insertion site of $argos^{W11}$, leading us to believe that this 2.8 kb cDNA did represent the *argos* transcription unit. S1 nuclease protection assays indicate that the point of insertion of the original enhancer trap element is within the 5′ untranslated region of this transcript.

We confirmed that this transcript, whose 5′ end is disrupted in all *argos* alleles, was also the one with the expression pattern detected by the $argos^{W11}$ enhancer trap, by comparing the expression pattern, as detected by tissue in situ hybridization, with that of the β-gal expression. These patterns, which are described below, were found to correspond well. On the basis of these results we conclude that these cDNAs represent the *argos* gene transcript.

The Expression of *argos*

The description of *argos* expression in the developing eye comes from the expression of the β-galactosidase reporter gene in the $argos^{W11}$ enhancer trap line, since in situ hybridizations to the eye disc were not precise enough to allow single-cell resolution, although they do show that the transcript is expressed behind the morphogenetic furrow (data not shown). *argos* is expressed in all developing photoreceptors and cone cells in the third instar eye imaginal disc (Figures 6A–6C). It first appears behind the morphogenetic furrow and is switched on strongly at about the same time as a cell first expresses neural antigens. Thus, *argos* appears in cells in the same order in which they differentiate: first cell R8, then cells R2 and R5, R3 and R4, R1 and R6, R7, and finally the cone cells. *argos* is not strongly expressed in the mystery cells, although we do detect a very low level of expression in all cells behind the furrow. In pupal retinae argos can be detected in cone cells, in photoreceptors (though more weakly than earlier in development), and in primary pigment cells (Figures 6D and 6E). It is not expressed in secondary or tertiary pigment cells, nor in the bristle cell groups. In the adult eye, *argos* is not expressed in photoreceptors, but is still expressed in a subset of the cells whose nuclei lie further apically than the photoreceptors, which are probably the cone cells (Figure 6F). *argos* is also expressed in a subset of cells in the optic lobes and the central brain.

The expression of *argos* in the embryo was examined by whole-mount in situ hybridization, and by histological detection of β-gal expression in the $argos^{W11}$ enhancer trap (Figures 6G–6L). *argos* transcripts are first detected in the cellular blastoderm and show a complex and dynamic pattern throughout most of the rest of embryonic development. Given the ventral expansion phenotype of *argos* mutations, it is significant that the gene is expressed in the ventral epidermis (for detailed description of *argos* embryonic expression, see legend to Figure 6).

The argos Protein Appears to Be Secreted

We sequenced the two longest cDNAs corresponding to the *argos* transcript. Conceptual translation of this sequence indicates that there is a single long open reading frame, which encodes a predicted protein of 444 aa (Figure 5B). Both the cDNAs that were sequenced contain in-frame stop codons prior to the beginning of the long open reading frame, indicating that the whole coding sequence is included in these clones. The *argos* sequence has a stretch of 22 hydrophobic residues, resembling a signal sequence, at its N-terminus, and no other region that is likely to span a membrane, indicating that it is probably a secreted protein (von Heijne, 1986). There are two potential N-linked glycosylation sites (Hubbard and Ivatt, 1981). The argos protein sequence is not closely related to any known protein. However, there is a cysteine-rich region that is reminiscent of an epidermal growth factor (EGF) repeat (see legend to Figure 5).

Discussion

Although *argos* mutations affect more than one aspect of Drosophila development, its role in the eye has provided us with the most insight into its function. Eye defects become apparent in *argos* mutants at an early stage: at the

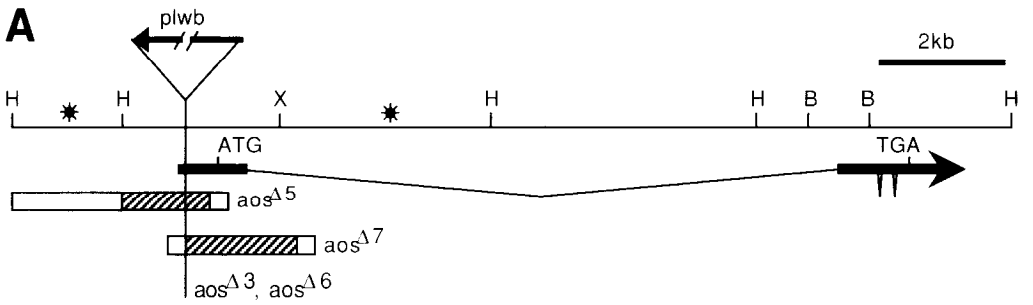

B

```
961  CTTCAACGGCTCTCGTTCGCCGGCGCCTGTTCGTTTTTGGATTTTCTGTTTGATCAGTTCGAAAAGTGAGTTGGTCGAGCGAACAACGATAGAGCGAGCGCAGAGTAACCGAGGCGATAC
1081 GATACGATATAATATAGCATCGGTACCATTGGGTATACGTTCCAGGAGCGAAAGAAAAGACGAAAACGAGACGAGACGAAAGGCCACCGGAGACAGCGACGTCGCGGGTGTTAAGTTACT
1201 AAATAGCAAACAGAAACTACCGACCACCGACCGATTGCAGTGAATGAAATATCCAATAATTTCGAGTGACATTGGCCACAAATCAATCGATCGTTCGATTTGAAACCTGATTTGTAGAGT
1321 TCGTTTCTGCCAGTGTGTGTGTGCATGTAAGCCATGGGTTCTGGGCGAGCGAGGGAGATAGAGCGAGAACACTGATTCGACTCGATTCGATTCGATTCGATTCGATTGGATTTGATTCGAATTCA
1441 ATTACAAAATTCATTGAGTGTCAATTACAAACCGCAAGAAAACAACACGCACGGAGATTCGGAAAGATCCCAAGATCCAAATACAAGATCCAGATCCAGATTCTCGAACATCCAGAGATC
1561 CCAGCCAGAGTCAGAGTCATAAATCATGCCTACGACATTGATGTTGCTGCCGTGCATGCTGCTGTTGCTGCTGACCGCCGCTGCCGTTGCTGTCGGCGGCACGCGACTGCCGCTCGAGGT
1    M P T T L M L L P C M L L L L T A A A V A V G G T R L P L E V

1681 GTTCGAGATTACGCCGACCACATCCACAGCGGACAAGCACAAGAGTCTGCAGTACACCGTCGTCTACGATGCCAAAGATATTTCAGGAGCAGCGGCAGCAACTGGAGTGGCGAGCAGTAC
41   F E I T P T T S T A D K H K S L Q Y T V V Y D A K D I S G A A A A T G V A S S T

1801 AGTGAAGCCCGCCACCGAGCAACTGACCGTTGTGAGCATTTCCTCCACAGCGGCTGCGGAGAAGGATCTCGCCGAGTCGCGGCGACATGCGCGACAAATGTTGCAGAAACAACAGCAGCA
81   V K P A T E Q L T V V S I S S T A A A E K D L A E S R R H A R Q M L Q K Q Q Q H

1921 TCGCAGCATCATCGGCGGCAAGCACGGCGATCGGGATGTGCGCATCCTCTACCAAGTGGGGGACTCTGAGGAGGATTTGCCCGTCTGTGCACCGAATGCAGTTTGCTCCAAGATCGATCT
121  R S I I G G K H G D R D V R I L Y Q V G D S E E D L P V C A P N A V C S K I D L

2041 ATACGAAACCCCGTGGATCGAGCGACAATGTCGTTGTCCTGAATCGAATCGCATGCCCAACAATGTGATCATCCATCATCACAGTCATTCCTCGGGATCGGTGGATTCCCTGAAGTACAG
161  Y E T P W I E R Q C R C P E S N R M P N N V I I H H H S H S S G S V D S L K Y R

2161 GAACTACTACGAAAGGGAGAAGATGATGCAGCACAAGCGAATGCTGTTGGGTGAATTTCAGGATAAGAAATTCGAAAGTCTGCATATGAAGAAGCTGATGCAGAAACTGGGCGCCGTCTA
201  N Y Y E R E K M M Q H K R M L L G E F Q D K K F E S L H M K K L M Q K L G A V Y

2281 CGAGGATGATTTGGATCATCTGGACCAGTCGCCGGACTATAATGACGCCCTGCCCTATGCGGAGGTGCAGGACAATGAGTTTCCCAGGGGATCGGCGCACATGAGGCATTCCGGGCACCG
241  E D D L D H L D Q S P D Y N D A L P Y A E V Q D N E F P R G S A H M R H S G H R

2401 AGGATCCAAAGAGCCTGCAACCACATTCATTGGCGGCTGTCCCAGCAGTTTGGGCGTGGAAGATGGCCACACCATTGCCGATAAGACTAGGCATTACAAAATGTGCCAGCCGGTGCATAA
281  G S K E P A T T F I G G C P S S L G V E D G H T I A D K T R H Y K M C Q P V H K

2521 GTTGCCAGTTTGCAAACACTTCCGTGACTACACTTGGACTTTGACAACAGCAGCCGAGTTGAATGTGACGGAGCAGATAGTCCATTGTCGGTGTCCCCGGAATTCGGTGACATACTTGAC
321  L P V C K H F R D Y T W T L T T A A E L N V T E Q I V H C R C P R N S V T Y L T

2641 CAAGAGGGAACCCATTGGCAATGACAGTCCGGGCTACAGATATCTGTTCGCCTGCTCTCCCCTGACGCGTCTTCGCTGTCAGCGAAAGCAACCGTGCAAATTGTTCACGGTGCGAAAGCG
361  K R E P I G N D S P G Y R Y L F A C S P L T R L R C Q R K Q P Ç K L F T V R K R

2761 CCAGGAGTTCCTGGACGAGGTCAACATTAACTCGTTGTGCCAGTGCCCCAAAGGACACCGCTGTCCCAGTCATCACACGCAATCCGGCGTGATAGCCGGCGAGAGTTTTCTGGAGGACAA
401  Q E F L D E V N I N S L C Q C P K G H R C P S H H T Q S G V I A G E S F L E D N

2881 CATACAGACATATTCCGGTTACTGCATGGCCAACGATTGAGTGCATCGCCCAGGGGATCATTCCACACATAATATATATAGAATACACTTTGTAAAGGAAGATAGAGTTGAGCGGAGGAG
441  I Q T Y S G Y C M A N D *

3001 CAACAGCTACTATATAGATATCGACTGAGCCAATTGAGTCTCGCCAAGTTACCAACTAATGAACTAATGAGAAGGGAAAAACGAACAAATACAAGCTAGGAACTTAAAATGCACTTCCAC
3121 ACAGATCATTTTGAAGTTTTTCAGAAAAAGAGAGAGAGAGCGTGTTTCTTTTGCTACCAAATTTTGGTCATAAAACGTATGATATAAATATTTAATTAGTTTTAAGCATCGATATGTGCG
3241 CAGTTTGTTATACAAATAATTTGTAATGAATATTTATGAAAACAAGAGCAAAACCTGCAACGAAGGAGGGCACTCCACTATGTAATATAGCAACAAACTATACTCGTAAACTAACCCGCA
3361 TAAATTGTATATATCTTTAATATATGTTTAACGAAAACAGTTTCGGTTATAATTTAAACGGAAATTACGCGGAGCAACGCAGCAAACGTCAAAGAGCAGGATGTGCCAAATGTTCAGATG
3481 GGGTGCACTTAGTTAACATAAGGATGTATCATTGAATAATTCATAGCGAAGGCAGTTTGAAACTGTGGCAACTCTGGCAGCTATTTTAGTGCAATTTTTGTGACGCCTTCACAGCCACTT
3601 CTCCGGAATTTGAGCAAGTAAATTAGAAATTAATTTAGAAATTGCGCAAAGGCTTTTAACTAAACGTATAGTAACCACCATGACTCCTCCTCTTCCCACTAAATTATGCATATGTACATC
3721 GATTTAAGCAACAAGATTTTGTTTATCTTAAAACGAGCAACGAACTTTGGCGATGTTTCGGTTTAAACACTTTGTAAAAAGGCAAAAATAAAAATTAATTTATGAACAAAAAAA
```

Figure 5. The Structure of the argos Gene

(A) A physical map of the *argos* region. The insertion site for the *argos*^{W11} enhancer trap element (which is approximately 13 kb) is indicated. The *lac-Z* gene is in the opposite transcriptional orientation from the *argos* gene. The extent of deletions in *argos* lethal mutants was analyzed by genomic DNA blotting and is indicated under the diagram of the transcript; hatched bars indicate sequence missing in the alleles, and uncertainty at the end of the deletions is indicated by open bars; *argos*$^{\Delta 3}$ and *argos*$^{\Delta 6}$ are internal deletions of the P element. Asterisks above the map show which other restriction fragments detected cDNAs. One class of cDNAs hybridized with the XbaI–HindIII fragment contained within the large intron; none of these cDNAs hybridized with any of the cDNAs from the *argos* gene, indicating that there may be a separate gene within the large intron. Another transcription unit was detected by the HindIII fragment to the left of the insertion fragment. These cDNAs extended beyond the leftmost HindIII site on this map, and none of them cross-hybridized with any *argos* cDNAs. B, BamHI; H, HindIII; X, XbaI.

(B) The sequence of the *argos* gene. This represents a composite of genomic and cDNA sequence. The two longest cDNAs were completely sequenced, and their 5′ ends are indicated at nt 1050 and 1055; both extend as far as the poly(A) tail. Restriction fragments from genomic DNA incorporating all the known exons of *argos* were also sequenced in order to confirm the cDNA sequence and to discover the intron/exon structure of the gene. DNA coordinates are measured from the HindIII site to the left of the insertion site (see A). Amino acid coordinates are measured from the first in-frame methionine; there are three closely spaced AUG codons, and we cannot predict which one is used to initiate translation. The position of the enhancer trap insertion is indicated by an open arrow and was ascertained by sequencing. The sequence highlighted by a black bar (GTTTGATCAG) indicates the 3′ extent of an S1 nuclease protected fragment of a complementary probe (5′ end of probe at nt 1167). This sequence overlaps with a good match to the consensus eukaryotic transcriptional start site (ATCAGTT) (Hultmark et al., 1986), so this may be the true 5′ end of the message. However, this sequence also forms part of a good consensus splice acceptor site, so this may indicate the presence of another 5′ exon, which would be entirely noncoding. There is no good TATA box upstream of this sequence. The positions of the three introns are indicated by black arrowheads in the sequence; the intron sizes are ≈9.5 kb, 68 bp, and 67 bp, respectively. There is a polyadenylation signal around coordinate 3810, which is underlined. The predicted signal sequence is shown with a dashed underline, and the potential N-linked glycosylation sites are circled. The EGF-like motif in the *argos* sequence is indicated by a solid underline. This sequence has the characteristic group of six cysteines, and the next most conserved residue, a glycine 3 aa C-terminal to the fifth cysteine. However, there is a longer gap between cysteines 3 and 4 than in any other EGF repeat (20 aa, compared with 7–10 usually), and there are some other quite well conserved residues that are absent from the *argos* sequence. We used the program BlastP (Altschul et al., 1990) to search existing databases with this EGF-like motif; although some EGF-repeat proteins were selected, their scores were poor. We also tried searching the databases with a short stretch of amino acids immediately flanking cysteines 4 and 5, as these appear to be the most conserved region within EGF repeats: in this case, seven proteins were selected—six have EGF motifs, and one did not but is cysteine rich. On the basis of these data, we remain uncertain about the functional significance of the EGF-like motif in *argos*.

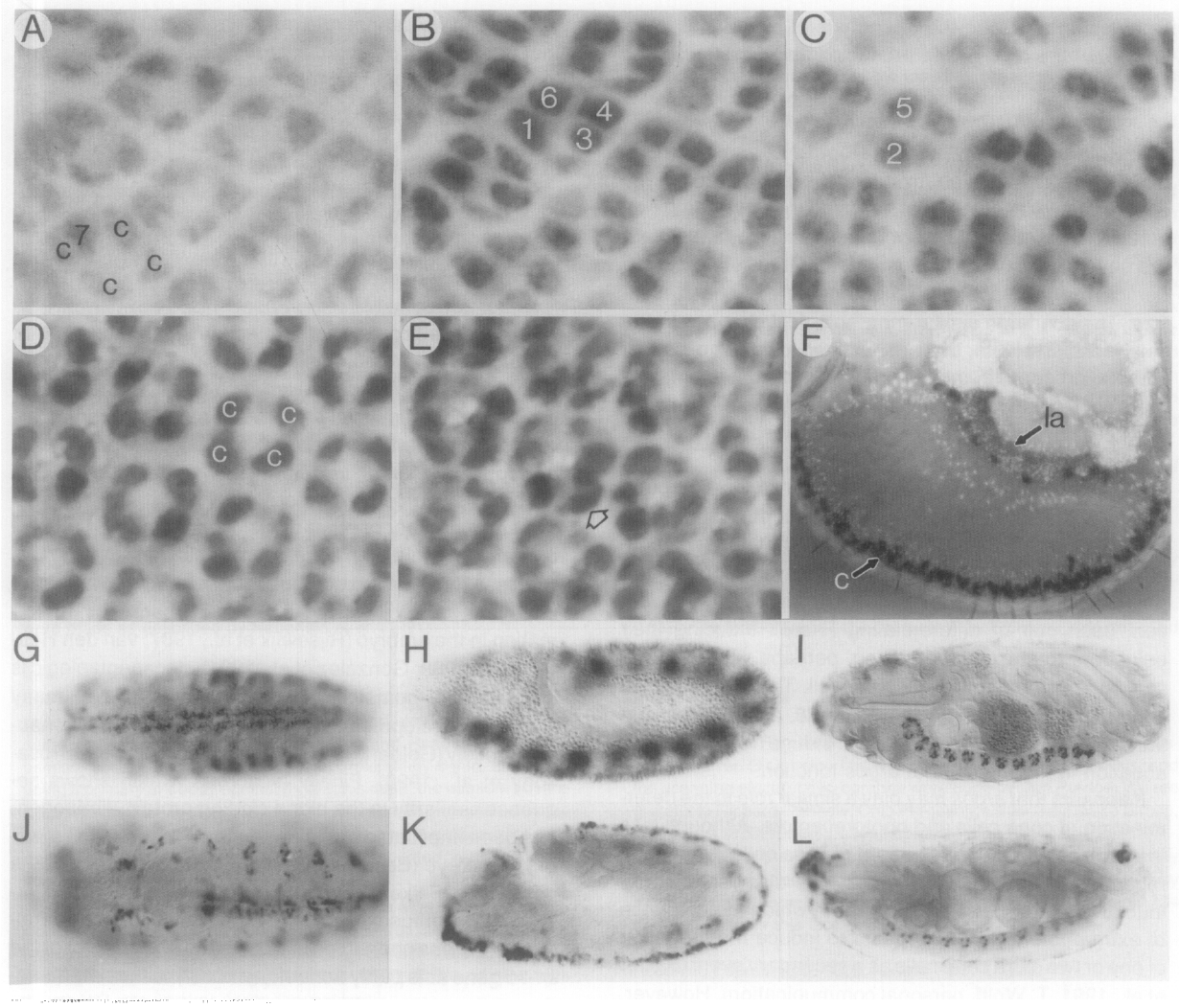

Figure 6. The Expression Pattern of *argos*

(A–F) The expression of the *argos*^{W11} enhancer trap in the developing eye, as detected by immunostaining against β-galactosidase, which is localized in the nucleus. (A)–(C) show three progressively more basal focal planes through a third instar eye imaginal disc. The morphogenetic furrow is to the bottom of each panel. In (A), the nuclei of the four cone cells and cell 7 are indicated; in (B), cells 1, 6, 3, and 4 are indicated; and in (C), cells 2 and 5; the nucleus of cell 8 lies just below the nuclei of cells 2 and 5, and is out of the plane of focus. (D) and (E) show two focal planes through a 40 hr pupal retina: (D) *argos* is expressed in cone cells (c), and (E) *argos* expression is seen in photoreceptors and in primary pigment cells; the arrow points to a primary pigment cell nucleus on the edge of a ring of photoreceptors. (F) shows a 10 μm cryostat section through an adult eye, which has been stained with the fluorescent nuclear dye, Hoechst 33258 (seen as white), and the X-Gal reaction product of the β-galactosidase histochemical reaction (seen as black). The major site of expression is in a subset of the most apical nuclei, which include those of the cone cells and some of the pigment cells; we believe this expression is in the cone cell nuclei (c). There is also expression in a subset of nuclei in the lamina (la). The photoreceptors are not stained.

(G–L) Embryonic *argos* expression: (G–I) whole-mount in situ hybridization, using an *argos* probe; (J–L) *argos*^{W11}/+ embryos immunostained with an antibody against β-galactosidase. Anterior is to the right. *argos* expression begins in the cellular blastoderm in two dorsal regions at the anterior end and one at the posterior end; there is also expression in a the dorsal ectoderm anlagen, in a segmental "pair-rule" type pattern. At the end of gastrulation (stage 9), the mesoderm has invaginated, and there are two rows of ectodermal cells bordering the mesectoderm that start to express *argos* RNA. As the mesectoderm invaginates, these two rows meet, and *argos* becomes expressed in the entire ventral ectoderm. It is not clear if this increase in *argos* expression is due to newly expressing cells or the division of already positive cells. In germband extended embryos (stage 10–11), additional expression in the head region and in unidentified segmentally repeated groups of ectodermal cells is apparent. (G) and (J) show a stage 11 embryo, ventral view (G) and dorsal view (J). (H) and (K) show a lateral view of a stage 11 embryo. Dorsal and lateral epidermal cells located at the segment boundary, and all ventral epidermal cells, express *argos* until stage 16. As the germband retracts, *argos* is expressed in the midline glial cells of the central nervous system. The onset of *argos* expression in these cells coincides with the onset of their posteriorly directed migration, and remains high throughout the rest of embryogenesis. (I) and (L) show a lateral view of a stage 17 embryo.

time that the first five photoreceptor neurons begin to differentiate, many of the mystery cells start to express neural antigens and continue to develop into mature photoreceptors. This contrasts with wild-type flies, in which the mystery cells leave the developing cluster and appear to rejoin the pool of uncommitted cells. Later, extra cone cells are recruited into the developing ommatidia, as well as extra primary pigment cells. Based on the ability of wild-

type tissue to rescue the phenotype of *argos*⁻ cells, we judge that the *argos* gene product is able to diffuse over several cell diameters.

The Role of *argos* in the Developing Eye

It is notable that it is the mystery cells, and not the many other uncommitted cells that surround the developing ommatidia, that adopt an inappropriate neural fate. There are several reasons to believe that the mystery cells are particularly susceptible to transformation into photoreceptors. They undergo similar morphological changes to the cells in the precluster that are destined to become the first five photoreceptors, they express sevenless protein, and there are several mutations apart from *argos* in which mystery cells become photoreceptors (Tomlinson et al., 1987; Mlodzik et al., 1990b; Fischer-Vize et al., 1992; Gaul et al., 1992). The mystery cells can therefore be thought of as arresting in some kind of "pre-photoreceptor" state, and the role of *argos* at that time may be in that arrest mechanism. Tomlinson and Ready (1987a) have proposed that photoreceptor determination occurs by successive induction, each pair of differentiating R cells inducing their neighbors to start differentiating, perhaps with a necessary role for contact with R8 as well. The mystery cells contact cells R3 and R4, as well as R8, and it is possible that these contacts are sufficient to induce neuronal differentiation in the absence of *argos* function.

It appears that *argos* may play a similar role in the determination of cone cells and photoreceptors. Although less is known about the development of cone cells than photoreceptors, it is believed that they are also recruited by inductive signals. There are cases in which the presence of extra photoreceptors appears to induce the formation of one or two extra cone cells as a secondary event (Basler et al., 1991; T. Wolff, personal communication). However, the one or two extra photoreceptors seen in *argos* ommatidia would not be expected to be sufficient to account for the recruitment of more than twice the normal number of cone cells, which is typical in *argos* pupal retinae. Therefore, we believe that *argos* has a primary function during cone cell determination as well as photoreceptor determination.

argos Mediates Communication between Cells

Our clonal analysis provides evidence that the *argos* protein is capable of diffusing and thereby influencing cell fate decisions over a range of several cell diameters. While this indicates that the protein is extracellular, and relatively free to diffuse, it is important to point out that this does not necessarily mean that it normally acts over such a range. The expression pattern of *argos* suggests that its level is high throughout the developing disc; furthermore, it is expressed in cells 3 and 4, which are adjacent to the mystery cells, so the effect of *argos* in the wild-type disc could be local. The genetic evidence that *argos* is a secreted protein is strongly supported by the molecular analysis of the gene. The predicted protein has a putative signal sequence and no other potential membrane-spanning domain (von Heijne, 1986), implying that it is secreted by the cell.

Although we cannot rule out there being subtle defects that we have not detected in *argos* discs, a possible working hypothesis about the function of *argos* is suggested by our data. Using a temperature-sensitive allele of the *Notch* gene, it has been shown that as each successive cell type is specified in the developing eye disc, more than the required number of cells are competent to adopt that particular fate (Cagan and Ready, 1989). The *argos* gene product may play a role in repressing inappropriate differentiation of these additional competent cells, at least during photoreceptor and cone cell recruitment. In this view, *argos* acts as a negative regulator of the inductive interactions that are thought to promote cell fate choices in the eye, with determination being controlled by a balance of opposing positive and negative signals. More extensive characterization of the earliest stages of ommatidial assembly will be required in order to determine whether this working hypothesis is broadly correct.

A small number of other diffusible proteins with roles in cell fate determination have been identified in Drosophila. wingless, which is homologous to the mammalian protooncogene *int-1*, is involved in regulating parasegment formation in the embryo (Rijsewijk et al., 1987; van den Heuvel et al., 1989; González et al., 1991). decapentaplegic is a Drosophila homolog of TGF-β; it functions at many stages of development, and has been shown to act nonautonomously (Gelbart, 1989; Panganiban et al., 1990; Posakony et al., 1990). Finally, scabrous, which shows sequence similarity to the blood clotting protein, fibrinogen, has been implicated in the regulation of ommatidial spacing in the eye (Baker et al., 1990). Although argos has a possible EGF-like repeat, it has no other significant similarity to known diffusible factors. There is an interesting parallel to the *argos* phenotype in C. elegans: the product of the *lin-15* gene acts partly nonautonomously in the determination of the vulva. In *lin-15* mutants additional vulval cells differentiate, and it has been proposed that the role of the gene is to repress inappropriate recruitment among competent cells (Herman and Hedgecock, 1990).

Concluding Remarks

In order to understand fully the mechanism by which *argos* operates in the eye, it will be necessary to characterize the phenotype more fully. It would also be useful to find the receptor through which it is likely to act, and the genetic and molecular techniques available in Drosophila should help this analysis. Few receptors for diffusible factors regulating cell determination have been identified (López-Casillas et al., 1991; Mathews and Vale, 1991; Wang et al., 1991; Attisano et al., 1992). Since *argos* appears to inhibit various cell types from differentiating inappropriately, the receptor should be expressed in at least those cells that *argos* represses, including the mystery cells. We have looked for a genetic interaction between *argos* and two potential candidates for a receptor, the Drosophila EGF receptor homolog (Baker and Rubin, 1989) and *Notch* (Cagan and Ready, 1989), but have not detected any specific effect. It should be possible to carry out a genetic screen for modifiers of *argos* mutations, thereby allowing us to identify interacting molecules, including the potential receptor.

Experimental Procedures

Fly Strains

The *argos*^{W11} mutation was isolated as a rough eye mutation from an enhancer trap screen; its cytological position is 73A3,4. Enhancer trapping was first described by O'Kane and Gehring (1987), and we followed the procedure described by Mlodzik and Hiromi (1992), but used the plwb element, which contains the *white* gene as a dominant marker (kindly provided by U. Grossniklaus and W. Gehring). The lethal alleles of *argos* were generated by excision of the enhancer trap P element. This was carried out by crossing *argos*^{W11} flies to flies carrying a stable source of P transposase (Robertson et al., 1988) and making homozygous lines from individuals that had lost the *white* marker.

Histology and Scanning Electron Microscopy of Adult Heads

Adult Drosophila heads were fixed and embedded in Durcupan resin essentially as described by Tomlinson and Ready (1987b), except that after removing the head and cutting off one eye to allow penetration of the fixative, the heads were initially fixed in 2% glutaraldehyde in 0.1 M phosphate buffer (pH 7.2) for 30 min on ice. Embedded heads were sectioned on a Reichert Jung microtome; 2 μm sections were dried onto slides, mounted in DPX (Fluka), and viewed under phase-contrast optics.

X-Gal staining of cryostat sections of adult heads was done as described by Fortini and Rubin (1990). Scanning electron micrographs were made as described by Heberlein et al. (1991).

Immunostaining Eye Imaginal Discs

Eye imaginal discs were dissected from third instar larvae in 0.1 M phosphate buffer (pH 7.2) and then fixed and stained by largely the same method as described by Tomlinson and Ready (1987a). The osmium postfixation was reduced to approximately 1 min, and when using a primary antibody against β-galactosidase, the osmium postfixation was omitted. In this case the DAB reaction was intensified by the addition of 0.1% $NiCl_2$ to the DAB–H_2O_2 mix, and the discs were then dehydrated through an ethanol series and mounted in methyl salicylate.

Primary antibodies used were 22C10 (Fujita et al., 1982), a monoclonal supernatant used at a dilution of 1:2; BP104, against neuroglian (Hortsch et al., 1990), a monoclonal supernatant used at 1:5; and anti-β-galactosidase (Promega), used at 1:500. A Biorad goat anti-mouse IgG was used as secondary antibody.

Cobalt Sulfide Staining of Pupal Retinae

Cobalt sulfide staining (Melamed and Trujillo-Cenoz, 1975) of staged pupal retinae was performed as described by Wolff and Ready (1991). Staging was carried out by aging white prepupae at 25°C.

Generation of Mitotic Clones

Mitotic clones of argos alleles were produced by the method described by Tomlinson et al. (1988). The dominant marker used was the P[w]33 element at cytogenetic position 70C (our unpublished data).

Embryonic Cuticle Preparations

Cuticle preparations were done according to the protocol of Wieschaus and Nüsslein-Volhard (1986). Embryos were removed from their vitelline membranes prior to fixation and were mounted in 1:1 Hoyer's mountant:lactic acid.

Molecular Cloning and DNA Manipulation

The genomic region surrounding the *argos* locus was isolated from an isogenic third chromosome genomic library (K. Moses, unpublished data). cDNAs were isolated from a λ gt10 library of third instar eye imaginal disc cDNA (A. Cowman and G. M. R., unpublished data), and from a 6–8 hr embryonic cDNA library made by Novagen in λ EXlox (Palazzolo et al., 1990).

All DNA and RNA manipulations, including subcloning, SI nuclease protection, and genomic DNA blotting, were done according to the protocols of Sambrook et al. (1989). The S1 nuclease protection probe was an M13 sequencing template, complementary to the coding strand, spanning the region where the 5′ end of the longest cDNA terminated.

The extent of four excision mutants, *argos*$^{\lambda 3}$, *argos*$^{\lambda 5}$, *argos*$^{\lambda 6}$, and *argos*$^{\lambda 7}$, was analyzed by genomic DNA blotting. Labeled probes from immediately on either side of the insertion site were used to find in which restriction fragments the breakpoints occur. In *argos*$^{\lambda 3}$ and *argos*$^{\lambda 6}$, both ends of the enhancer trap P element are still present, and there is no disruption of restriction fragments in the flanking DNA. This indicates that these two alleles are internal deletions within the P element. *argos*$^{\lambda 5}$ removes DNA on either side of the insertion site, and thus removes the entire P element: the left end of the deletion is within the 1.85 kb HindIII fragment to the left of the insertion site, and the right end of the deletion lies between an EcoRI site at base 1434 on our map (Figure 5A) and a PstI site at base 1729. *argos*$^{\lambda 7}$ is a deletion almost entirely to the right of the insertion. The entire P element is removed, and there is either a clean excision at the left end, or else a deletion of less than 300 bp to the left of the insertion; the right end of the deletion lies less than 300 bp to the right of an EcoRI site, which is itself approximately 300 bp to the right of the XbaI site indicated in Figure 5A. Therefore, *argos*$^{\lambda 7}$ removes all of the 5′ exon, including the N-terminal 140 aa.

Sequencing was performed by the chain termination method of Sanger et al. (1977), using Sequenase (U.S. Biochemicals).

Embryo In Situ Hybridization and Immunocytochemistry

Nonradioactive in situ hybridizations to embryos were carried out by the digoxygenin method described by Tautz and Pfeifle (1989). Immunostaining of embryos was performed by the method of Patel et al. (1987). The antibody against β-gal is made by Promega, and was used at a dilution of 1:500.

Acknowledgments

We thank Chip Ferguson and Tanya Wolff for many helpful discussions; Warren Gish helped us with computer sequence analysis; and the scanning electron micrographs were done by Don Pardoe. We are grateful to Richard Carthew, Chip Ferguson, Ulrike Gaul, Mike Simon, and Tanya Wolff for their useful comments on this manuscript.

The costs of publication of this article were defrayed in part by the payment of page charges. This article must therefore be hereby marked "*advertisement*" in accordance with 18 USC Section 1734 solely to indicate this fact.

Received February 19, 1992; revised April 7, 1992.

References

Altschul, S. F., Gish, W., Miller, W., Myers, E. W., and Lipman, D. J. (1990). Basic local alignment search tool. J. Mol. Biol. *215*, 403–410.

Amaya, E., Musci, T. J., and Kirschner, M. W. (1991). Expression of a dominant negative mutant of the FGF receptor disrupts mesoderm formation in Xenopus embryos. Cell *66*, 257–270.

Artavanis-Tsakonas, S. and Simpson, P. (1991). Choosing a cell fate: a view from the *Notch* locus. Trends Genet. *7*, 403–408.

Attisano, L., Wrana, J. L., Cheifetz, S., and Massagué, J. (1992). Novel activin receptors: distinct genes and alternative mRNA splicing generate a repertoire of serine/threonine kinase receptors. Cell *68*, 97–106.

Baker, N. E. (1987). Molecular cloning of sequences from *wingless*, a segment polarity gene in *Drosophila*: the spatial distribution of a transcript in embryos. EMBO J. *6*, 1765–1773.

Baker, N. E., and Rubin, G. M. (1989). Effect on eye development of dominant mutations in *Drosophila* homologue of the EGF receptor. Nature *340*, 150–153.

Baker, N. E., Mlodzik, M., and Rubin, G. M. (1990). Spacing differentiation in the developing *Drosophila* eye: a fibrinogen-related lateral inhibitor encoded by *scabrous*. Science *250*, 1370–1377.

Basler, K., Christen, B., and Hafen, E. (1991). Ligand-independent activation of the *sevenless* receptor tyrosine kinase changes the fate of cells in the developing Drosophila eye. Cell *64*, 1069–1081.

Bier, E., Ackerman, L., Barbel, S., Jan, L., and Jan, Y. N. (1988). Identification and characterisation of a neuron-specific nuclear antigen in *Drosophila*. Science *240*, 913–916.

Cagan, R. L., and Ready, D. F. (1989). *Notch* is required for successive

cell decisions in the developing *Drosophila* retina. Genes Dev. *3*, 1099–1112.

Campos, A. R., Fishbach, K.-F., and Steller, H. (1992). Survival of photoreceptor neurons in the compound eye of *Drosophila* depends on connections with the optic ganglia. Development *114*, 355–366.

Cohen, B., Wimmer, E. A., and Cohen, S. M. (1991). Early development of leg and wing primordia in the *Drosophila* embryo. Mech. Dev. *33*, 229–240.

Daniels, S. B., McCarron, M., Love, C., and Chovnick, A. (1985). Dysgenesis-induced instability of *rosy* locus transformation in *Drosophila melanogaster*: analysis of excision events and the selective recovery of control element deletions. Genetics *109*, 95–117.

Fischer-Vize, J. A., Vize, P., and Rubin, G. M. (1992). A unique mutation in the *Enhancer of split* gene complex affects the fates of the mystery cells in the developing *Drosophila* eye disc. Development, in press.

Fortini, M. E., and Rubin, G. M. (1990). Analysis of cis-acting requirements of the Rh3 and Rh4 genes reveals a bipartite organization to rhodopsin promoters in *Drosophila melanogaster*. Genes Dev. *4*, 444–463.

Fujita, S. C., Zipursky, S. L., Benzer, S., Ferrus, A., and Shotwell, S. L. (1982). Monoclonal antibodies against the *Drosophila* nervous system. Proc. Natl. Acad. Sci. USA *79*, 7929–7933.

Gaul, U., Mardon, G., and Rubin, G. M. (1992). A putative Ras GTPase activating protein acts as a negative regulator of signaling by the Sevenless receptor tyrosine kinase. Cell *68*, 1007–1019.

Gelbart, W. M. (1989). The *decapentaplegic* gene: a TGF-β homologue controlling pattern formation in *Drosophila*. Development *107* (suppl.), 65–74.

González, F., Swales, L., Bejsovec, A., Skaer, H., and Martinez Arias, A. (1991). Secretion and movement of *wingless* protein in the epidermis of the *Drosophila* embryo. Mech. Dev. *35*, 43–54.

Hafen, E., Basler, K., Edstroem, J. E., and Rubin, G. M. (1987). *sevenless*, a cell-specific homeotic gene of *Drosophila*, encodes a putative transmembrane receptor with a tyrosine kinase domain. Science *236*, 55–63.

Heberlein, U., Mlodzik, M., and Rubin, G. M. (1991). Cell-fate determination in the developing *Drosophila* eye: role of the *rough* gene. Development *112*, 703–712.

Herman, R. K., and Hedgecock, E. M. (1990). Limitation of the size of the vulval primordium of *Caenorhabditis elegans* by *lin-15* expression in surrounding hypodermis. Nature *348*, 169–171.

Hortsch, M., Bieber, A. J., Patel, N. H., and Goodman, C. S. (1990). Differential splicing generates a nervous system-specific form of Drosophila neuroglian. Neuron *4*, 697–709.

Horvitz, H. R., and Sternberg, P. W. (1991). Multiple intercellular signalling systems control the development of the *Caenorhabditis elegans* vulva. Nature *351*, 535–541.

Hubbard, S. C., and Ivatt, R. J. (1981). Synthesis and processing of asparagine-linked oligosaccharides. Annu. Rev. Biochem. *50*, 555–583.

Hultmark, D., Klemenez, R., and Gehring, W. (1986). Translational and transcriptional control elements in the untranslated leader of the heat-shock gene *hsp22*. Cell *44*, 429–438.

Krämer, H., Cagan, R. L., and Zipursky, S. L. (1991). Interaction of *bride of sevenless* membrane-bound ligand and the *sevenless* tyrosine-kinase receptor. Nature *352*, 207–212.

Lawrence, P. A., and Green, S. M. (1979). Cell lineage in the developing retina of *Drosophila*. Dev. Biol. *71*, 142–152.

López-Casillas, F., Cheifetz, S., Doody, J., Andres, J. L., Lane, W. S., and Massagué, J. (1991). Structure and expression of the membrane proteoglycan betaglycan, a component of the TGF-β receptor system. Cell *67*, 785–795.

Mathews, L. S., and Vale, W. W. (1991). Expression cloning of an activin receptor, a predicted transmembrane serine kinase. Cell *65*, 973–982.

Melamed, J., and Trujillo-Cenoz, O. (1975). The fine structure of the eye imaginal disc in muscoid flies. J. Ultrastruct. Res. *51*, 79–93.

Mlodzik, M., and Hiromi, Y. (1992). The enhancer trap method in *Drosophila*: its application to neurobiology. In Gene Expression in Neural Tissues (Methods in Neuroscience *9*), P. M. Cann, ed. (Orlando, Florida: Academic Press), pp. 397–414.

Mlodzik, M., Baker, N. E., and Rubin, G. M. (1990a). Isolation and expression of *scabrous*, a gene regulating neurogenesis in *Drosophila*. Genes Dev. *4*, 1848–1861.

Mlodzik, M., Hiromi, Y., Weber, U., Goodman, C. S., and Rubin, G. M. (1990b). The Drosophila *seven-up* gene, a member of the steroid receptor gene superfamily, controls photoreceptor cell fates. Cell *60*, 211–224.

O'Kane, C. J., and Gehring, W. J. (1987). Detection *in situ* of genomic regulatory elements in *Drosophila*. Proc. Natl. Acad. Sci. USA *84*, 9123–9127.

Palazzolo, M. J., Hamilton, B. A., Ding, D., Martin, C. H., Mead, D. A., Mierendorf, R. C., Raghavan, K. V., Meyerowitz, E. M., and Lipshitz, H. D. (1990). Phage lambda cDNA cloning vectors for subtractive hybridization, fusion-protein synthesis and *Cre-loxP* automatic plasmid subcloning. Gene *88*, 25–36.

Panganiban, G. E. F., Reuter, R., Scott, M. P., and Hoffmann, F. M. (1990). A *Drosophila* growth factor homolog, *decapentaplegic*, regulates homeotic gene expression within and across germ layers during midgut morphogenesis. Development *110*, 1041–1050.

Patel, N., Snow, P. M., and Goodman, C. S. (1987). Characterization and cloning of fasciclin III: a glycoprotein expressed on a subset of neurons and axon pathways in Drosophila. Cell *48*, 975–988.

Posakony, L. G., Raftery, L. A., and Gelbart, W. M. (1990). Wing formation in *Drosophila melanogaster* requires *decapentaplegic* gene function along the anterior–posterior compartment boundary. Mech. Dev. *33*, 69–82.

Ray, R. P., Arora, K., Nüsslein-Volhard, C., and Gelbart, W. M. (1991). The control of cell fate along the dorsal–ventral axis of the *Drosophila* embryo. Development *113*, 35–54.

Ready, D. (1989). A multifaceted approach to neural development. Trends Neurosci. *12*, 102–110.

Rijsewijk, F., Schuermann, M., Wagenaar, E., Parren, P., Weigel, D., and Nusse, R. (1987). The Drosophila homolog of the mouse mammary oncogene *int-1* is identical to the segment polarity gene *wingless*. Cell *50*, 649–657.

Robertson, H. M., Preston, C. R., Phillis, R. W., Johnson-Schlitz, D. M., Benz, W. K., and Engels, W. R. (1988). A stable genomic source of P element transposase in *Drosophila melanogaster*. Genetics *118*, 461–470.

Robinow, S., and White, K. (1991). Characterisation and spatial distribution of the ELAV protein during *Drosophila melanogaster* development. J. Neurobiol. *22*, 443–461.

Sambrook, J., Fritsch, E. F., and Maniatis, T. (1989). Molecular Cloning: A Laboratory Manual, 2nd ed. (Cold Spring Harbor, New York: Cold Spring Harbor Laboratory).

Sanger, F., Nicklen, S., and Coulson, A. (1977). DNA sequencing with chain terminating inhibitors. Proc. Natl. Acad. Sci. USA *74*, 5463–5467.

Smith, J. C., Price, B. M. J., van Nimmen, K., and Huylebroeck, D. (1990). Identification of a potent *Xenopus* mesoderm-inducing factor as a homologue of activin A. Nature *345*, 729–731.

Tautz, D., and Pfeifle, C. (1989). A non-radioactive *in situ* hybridization method for the localization of specific RNAs in *Drosophila* embryos reveals translational control of the segmentation gene *hunchback*. Chromosoma *98*, 81–85.

Tomlinson, A. (1988). Cellular interactions in the developing *Drosophila* eye. Development *104*, 183–193.

Tomlinson, A., and Ready, D. F. (1987a). Neuronal differentiation in the *Drosophila* ommatidium. Dev. Biol. *120*, 366–376.

Tomlinson, A. and Ready, D. F. (1987b). Cell fate in the *Drosophila* ommatidium. Dev. Biol. *123*, 264–275.

Tomlinson, A., Bowtell, D. D., Hafen, E., and Rubin, G. M. (1987). Localization of the *sevenless* protein, a putative receptor for positional information, in the eye imaginal disc of Drosophila. Cell *51*, 143–150.

Tomlinson, A., Kimmel, B. E., and Rubin, G. M. (1988). *rough*, a Drosophila homeobox gene required in photoreceptors R2 and R5 for inductive interactions in the developing eye. Cell *55*, 771–784.

van den Eijnden-van Raaij, A. J. M., van Zoelent, E. J. J., van Nimmen, K., Koster, C. H., Snoek, G. T., Durston, A. J., and Huylebroeck, D. (1990). Activin-like factor from *Xenopus laevis* cell line responsible for mesoderm induction. Nature *345*, 732–734.

van den Heuvel, M., Nusse, R., Johnston, P., and Lawrence, P. A. (1989). Distribution of the *wingless* gene product in Drosophila embryos: a protein involved in cell–cell communication. Cell *59*, 739–749.

von Heijne, G. (1986). A new method for predicting signal sequence cleavage sites. Nucl. Acids Res. *14*, 4683–4690.

Wang, X.-F., Lin, H. Y., Ng-Eaton, E., Downward, J., Lodish, H. F., and Weinberg, R. A. (1991). Expression cloning and characterization of the TGF-β type III receptor. Cell *67*, 797–805.

Wieschaus, E., and Nüsslein-Volhard, C. (1986). Looking at embryos. In *Drosophila*: A Practical Approach, D. B. Roberts, ed. (Oxford: IRL Press), pp. 199–227.

Wolff, T., and Ready, D. F. (1991). Cell death in normal and rough eye mutants of *Drosophila*. Development *113*, 825–839.

GenBank Accession Number

The accession number for the sequence reported in this paper is M91381.